Geometric Invariant Shape Representations using Morphological Multiscale Analysis.

L.Alvarez, L.Mazorra and F.Santana
Departamento de Informática y Sistemas
Universidad de Las Palmas de Gran Canaria
Campus de Tafira, 35017 Las Palmas, Spain
WWW: http://serdis.dis.ulpgc.es/ami

February 2001

Abstract

In this paper, we present a new geometric invariant shape representation using morphological multiscale analysis. The geometric invariant is based on the surface and perimeter evolution of the shape under the action of a morphological multiscale analysis. First, we present some theoretical results on the perimeter and surface evolution across the scales of a shape. In the case of similarity transformations, the proposed geometric invariant is based on a scale-normalized evolution of the isoperimetric ratio of the shape. In the case of general affine geometric transformations the proposed geometric invariant is based on a scale-normalized evolution of the surface. We present some numerical results to evaluate the performance of the proposed models.

1 Introduction.

Shape representation methods play an important role in systems for object recognition and analysis. According to the classification of shape analysis methods proposed by Pavlidis [11] and Loncaric [8], by shape representation methods we mean methods which provide a non-numeric representation of the shape (e.g. a graph). Shape description refers to the methods that result in a numeric descriptor of the shape and could be a step subsequent to shape representation. Another classification of shape

analysis methods is based on the use of shape boundary points as opposed to the interior of the shape. The two resulting classes of methods are known as boundary (also called external) and global (also called internal), respectively.

In the last years, multiscale analysis has became a common tool for many tasks in computer vision. A multiscale analysis can be defined as an operator $T_t(f)$ which provides for an original image f a sequence of images $T_t(f)$ which represent the image at a coarse scale t.

In this paper we deal with morphological multiscale analysis, which satisfy the morphological invariance, that is, the multiscale analysis $T_t(f)$ commutes with any increasing histogram modification of the image. It means that for any increasing function $g(.)$

$$T_t(f) \circ g = T_t(f \circ g)$$

the underlying hypothesis associated to this morphological invariance is that the contrast between the different objects present in the image is not important at all, and that all the information present in the image is described by the geometry of the level sets of the image. In particular, the way a shape changes under the action of a morphological multiscale analysis depends only of the geometry of its boundary.

The main goal of this paper is to enjoy of the nice geometric and morphological invariant properties of the morphological multiscale analysis in order to find out a reliable global shape representation. Linear scale-space shape representations have been studied by different authors in the literature: Witkin [13] proposed a scale space filtering approach by tracking the position of the inflection points in signals filtered by gaussians. Asada and Brady [4] proposed a representation called *the curvature primal sketch.* The shape boundary is filtered with gaussian functions of increasing width to obtain a boundary curvature-based multiscale representation of the shape. Mokhtarian and Mackworth [10] also propose a scale-space boundary shape representation based on the curvature evolution across the scales. In the context of the morphological scale spaces, Maragos [9] proposed the pattern spectrum representation based on the surface evolution of a shape obtained by opening the shape with a disk of increasing size. Cohignac et al., [5] and [6], proposed a method for affine invariant shape recognition based on the affine invariant morphological multiscale analysis. They use the multiscale analysis to recover characteristic points in the shape. Lisani et al. [7], use the affine invariant multiscale analysis to smooth the images before a local encoding of the shape elements.

The method proposed in this paper uses the evolution of the surface and/or perimeter of the shape across the scales using different morphological multiscale analysis as basic tools to find out scale-space global shape representation.

As it was proved by Alvarez, Guichard, Lions and Morel in [2], under some minimal architectural assumptions, all the morphological and euclidean invariant multiscale

analysis are generated by the partial differential equation:

$$\frac{\partial u}{\partial t} = \beta(curv(u)) \, \|\nabla u\| \tag{1}$$

where $\beta(.)$ is a nondecreasing function and $curv(u)(x, y)$ is the curvature of the level line passing by the point (x, y), that is:

$$curv(u) = div\left(\frac{\nabla u}{\|\nabla u\|}\right)$$

Therefore if $u(t, x, y)$ is the solution of equation (1), for the initial datum f, then

$$u(t, x, y) = T_t(f)(x, y)$$

We notice that these morphological multiscale analysis are invariant by euclidean and symmetry transformations $((x, y) \to (\pm x, \pm y))$.

Following the morphological principle, we will consider that a shape S_0 is given by a level set of the image f, that is:

$$S_0 = \overline{\{(x, y) : \ f(x, y) < \lambda\}}$$

for some λ, where for a set A, we denote by $\overline{A}$ the closure of A, that is, the minimum closed set including A. We will denote by $S(t)$ the evolution across the scales of S_0, that is:

$$S(t) = \overline{\{(x, y) : \ T_t(f)(x, y) < \lambda\}}$$

we will also denote by $C(t)$ the boundary of $S(t)$. In the case that $C(t)$ be a family of single Jordan curves, we can interpret the evolution of $C(t)$ in terms of curve evolution. In fact, $C(t)$ is a solution of the curve evolution equation

$$\frac{\partial C}{\partial t} = \beta(k)\vec{N} \tag{2}$$

where $\vec{N}$ represents the unit inward normal direction to the curve $C(t)$ and k is the curvature.

We point out that the function $|S(t)| = Surface(S(t))$ and $|C(t)| = Perimeter(C(t))$ are euclidean invariants of S_0. Indeed, since the multiscale analysis (1) is invariant

under euclidean transformations, given 2 shapes S_0, S_0', and $S(t)$, $S'(t)$ its corresponding evolutions, such that there exists an euclidean transformation E satisfying $S_0' = E(S_0)$, then

$$|S(t)| = |S'(t)| \quad for\ any\ t > 0$$
$$|C(t)| = |C'(t)| \quad for\ any\ t > 0$$

therefore the function $t \to |S(t)|$ and $t \to |C(t)|$ are euclidean invariants of the shape S_0.

The mathematical justification of some of the results that we are going to use here have been developed by Alvarez-Blanc-Mazorra and Santana in [1].

The organization of the paper is as follows: In section 2, we present some theoretical results on the surface and perimeter evolution of a shape under the action of a morphological multiscale analysis. In section 3, we analyze the similarity invariant shape representation, in this case we propose as geometric invariant a scale-normalized isoperimetric ratio evolution. In section 4, we study the affine invariant shape representation, in this case we propose as geometric invariant a scale-normalized surface ratio evolution. In section 5, we present some numerical experiences. In section 6 we present some conclusions.

2 Surface and perimeter evolution of a shape under the action of a morphological multiscale analysis

In this section, we will show formulas of the evolution of perimeter and surface following the equation (1). We will assume that $C(t)$, the boundary of the shape $S(t)$ at scale t, is a family of single Jordan curves.

Proposition 1 *If $C(t)$ is a family of singles Jordan curves, then the evolution across the scales of the length of the curve $|C(t)|$ under the action of (1), is given by*

$$\frac{\partial |C(t)|}{\partial t} = -\int_0^{|C(t)|} k\beta(k) ds, \tag{3}$$

with s the arclength along the curve.

Proof : see [1].

Remark : In the case of $\beta(k)$ be constant ($\beta(k) \equiv M$), we have:

$$\frac{\partial |C(t)|}{\partial t} = -M \int_0^{|C(t)|} k ds = -2\pi M$$

and therefore:

$$|C(t)| = |C(0)| - 2\pi M t$$

so in particular, in this case, the evolution of the perimeter $|C(t)|$ does not depend on the geometry of $C(t)$, and then, for this particular choice of $\beta(s)$, $|C(t)|$ can not be used to discriminate between different shapes.

Proposition 2 *If $C(t)$ is a family of singles Jordan curves, then the evolution across the scales of the surface $|S(t)|$ under the action of (1), is given by*

$$\frac{\partial |S(t)|}{\partial t} = -\int_0^{|C(t)|} \beta(k) ds. \tag{4}$$

Proof : See [1].

Remark : In the case of $\beta(k) = k$ we have:

$$\frac{\partial |S(t)|}{\partial t} = -\int_0^{|C(t)|} k ds = -2\pi$$

and therefore:

$$|S(t)| = |S_0| - 2\pi t$$

so in particular, in this case, the evolution of the surface $|S(t)|$ does not depend on the geometry of $C(t)$, and then, $|S(t)|$ can not be used to discriminate between different shapes. We notice that this result is true only for the particular choice $\beta(s) = s$, and that in general, for other values of $\beta(s)$ the evolution of the surface depends on the geometry of S_0.

3 Morphological Similarity Invariant Representation of a Shape.

In this section, we are going to study how to find out similarity invariant using the surface and perimeter evolution of $S(t)$. A similarity transformation H is generated by rotations, translations and isotropic scalings, and it can be expressed in the following way:

$$H(x,y) = k \begin{pmatrix} \cos(\alpha) & \sin(\alpha) \\ -\sin(\alpha) & \cos(\alpha) \end{pmatrix} \begin{pmatrix} x \\ y \end{pmatrix} + \begin{pmatrix} a \\ b \end{pmatrix}$$

We will say that a multiscale analysis is invariant under similarity transformations if for any transformation H, there exists a function $t \rightarrow t'(H,t)$ such that

$$H\left(T_{t'(H,t)}(f)\right) = T_t(H(f))$$

First at all, we are going to characterize the morphological multiscale analysis invariant under similarity transformation.

Proposition 3 *Let be $T_t(f)$ a morphological multiscale analysis given by (1). $T_t(f)$ is invariant under similarity transformations if and only if there exists a constant $p \geq 0$ such that:*

$$\beta(s) = \begin{cases} \beta(1)s^p & if \quad s \geq 0 \\ \beta(-1)(-s)^p & if \quad s < 0 \end{cases} \tag{5}$$

Moreover if k is the scaling factor of the similarity H, then

$$t'(H,t) = k^{p+1}t$$

Proof: See [1].

Remark: we notice that following the previous proposition the multiscale analysis $T_t(f)$ is not scale invariant in the sense that a similarity transformation does not modified the space and scale variables in the same way, it means that if we apply a zoom $(x,y) \rightarrow (kx,ky)$ to the shape, then the scale is modified by $t \rightarrow k^{p+1}t \neq kt$. In order to have the scale invariant property we need just to replace t by the transformation:

$$\tilde{t} = (t(p+1))^{\frac{1}{p+1}} \tag{6}$$

with the new scale $\tilde{t}$ we have that $(x, y, \tilde{t}) \rightarrow (kx, ky, k\tilde{t})$ under the action of the similarity transformation $H(x, y) = (kx, ky)$. Indeed,

$$H(T_{\tilde{tk}}(f)) = H(T_{\frac{(tk)^{p+1}}{p+1}}(f)) = T_{\frac{(t)^{p+1}}{p+1}}(H(f)) = T_{\tilde{t}}(H(f))$$

The new scale variable $\tilde{t}$ has a more physical meaning, for instance a disk of radius R_0 vanishes in a scale proportional to $\tilde{t} = R_0$. In the particular case of $\beta_1 = 1$, the vanishing scale of a circle is equal to its radius, so we can interpret that in a scale $\tilde{t}$, all the objects initially included in a disk of radius $\tilde{t}$ have been removed by the multiscale analysis.

Remark: We notice that, in fact, the similarity invariant morphological multiscale analysis depends on 3 parameters, the power $p \geq 0$ and the constant $\beta_{-1} = \beta(-1)$ and $\beta_1 = \beta(1)$ which are not completely free because the function $\beta(s)$ has to be nondecreasing. It means that if $p > 0$ then $\beta_1 \geq 0$ and $\beta_{-1} \leq 0$. In what follows we will represent the similarity invariant multiscale analysis $T_t(f)$ by these 3 parameters, that is :

$$T_t(f) = T_t^{(p,\beta_{-1},\beta_1)}(f)$$

we will use also the notation

$$S_{(p,\beta_{-1},\beta_1)}(t)$$
$$C_{(p,\beta_{-1},\beta_1)}(t)$$

to indicate the evolution of the shape S_0 and its boundary C_0 following the multiscale analysis given by (p, β_{-1}, β_1).

Among the different possibilities of similarity invariant morphological multiscale analysis let us mention 3 examples which correspond to some particular choices for (p, β_{-1}, β_1). The first example is given for the classical mathematical morphology operators dilation and erosion, which corresponds to the choices

$$(p, \beta_{-1}, \beta_1) = (0, 1, 1) \tag{7}$$
$$(p, \beta_{-1}, \beta_1) = (0, -1, -1) \tag{8}$$

The second example of multiscale analysis is given by the mean curvature motion operator, where we have typically 3 options for the choices of (p, β_{-1}, β_1):

$$(p, \beta_{-1}, \beta_1) = (1, -1, 1) \tag{9}$$
$$(p, \beta_{-1}, \beta_1) = (1, 0, 1)$$
$$(p, \beta_{-1}, \beta_1) = (1, -1, 0)$$

The third example of multiscale analysis that we consider is based on the affine invariant multiscale analysis discovered by Alvarez-Lions-Guichard-Morel [2] and Sapiro-Tannenbaum [12] in an independent way. In this case, we will use, again, 3 different choices for (p, β_{-1}, β_1):

$$\begin{aligned}(p, \beta_{-1}, \beta_1) &= (\frac{1}{3}, -1, 1) \\ (p, \beta_{-1}, \beta_1) &= (\frac{1}{3}, 0, 1) \\ (p, \beta_{-1}, \beta_1) &= (\frac{1}{3}, -1, 0)\end{aligned} \tag{10}$$

The scale-normalized isoperimetric ratio evolution.

In order to find out similarity invariants we have to normalize the scale following the scaling factor k. First we notice that if $T_t^{(p,\beta_{-1},\beta_1)}(f)$ is a morphological multiscale analysis invariant under similarity transformations, S_0, S_0' bounded shapes and H a similarity transformation such that $H(S_0') = S_0$, then using proposition 3, and (6) we obtain

$$\begin{aligned}S_{(p,\beta_{-1},\beta_1)}(\tilde{t}) &= H(S'_{(p,\beta_{-1},\beta_1)}(k\tilde{t})) \quad for\ any\ t \geq 0 \\ \left|S_{(p,\beta_{-1},\beta_1)}(\tilde{t})\right| &= \frac{\left|S'_{(p,\beta_{-1},\beta_1)}(k\tilde{t})\right|}{k^2} \quad for\ any\ t \geq 0 \\ \left|C_{(p,\beta_{-1},\beta_1)}(\tilde{t})\right| &= \frac{\left|C'_{(p,\beta_{-1},\beta_1)}(k\tilde{t})\right|}{k} \quad for\ any\ t \geq 0\end{aligned} \tag{11}$$

We will use as similarity invariant of a bounded shape S_0 the scale-normalized isoperimetric ratio evolution $I^{S_0}_{(p,\beta_{-1},\beta_1)}(\tilde{t})$ given by:

Definition 4 *Let be S_0 a bounded shape, we define the scale-normalized isoperimetric ratio evolution $I^{S_0}_{(p,\beta_{-1},\beta_1)}(\tilde{t})$ as the function*

$$I^{S_0}_{(p,\beta_{-1},\beta_1)}(\tilde{t}) = 4\pi \frac{\left|S_{(p,\beta_{-1},\beta_1)}(\tilde{t}\sqrt{|S_0|})\right|}{\left|C_{(p,\beta_{-1},\beta_1)}(\tilde{t}\sqrt{|S_0|})\right|^2}$$

We notice that $I^{S_0}_{(p,\beta_{-1},\beta_1)}(\tilde{t}) \leq 1$, and $I^{S_0}_{(p,\beta_{-1},\beta_1)}(\tilde{t}) = 1$ only in the case that $S_{(p,\beta_{-1},\beta_1)}(\tilde{t}\sqrt{|S_0|})$ be a circle. Next, we will show that $I^{S_0}_{(p,\beta_{-1},\beta_1)}(\tilde{t})$ is a similarity invariant of the shape S_0.

Theorem 5 *Let $T_t^{(p,\beta_{-1},\beta_1)}(f)$ be a morphological multiscale analysis invariant under similarity transformations, 2 bounded shapes S_0, S_0', such that there exists a similarity transformation H with $H(S_0') = S_0$, Then:*

$$I^{S_0}_{(p,\beta_{-1},\beta_1)}(\tilde{t}) = I^{S_0'}_{(p,\beta_{-1},\beta_1)}(\tilde{t}) \quad for\ \tilde{t} \geq 0$$

Proof: Let k be the scaling factor of the transformation H, using (11) we obtain:

$$I^{S_0}_{(p,\beta_{-1},\beta_1)}(\tilde{t}) = 4\pi \frac{\left|S_{(p,\beta_{-1},\beta_1)}(\tilde{t}\sqrt{|S_0|})\right|}{\left|C_{(p,\beta_{-1},\beta_1)}(\tilde{t}\sqrt{|S_0|})\right|^2} = 4\pi \frac{\left|S'_{(p,\beta_{-1},\beta_1)}(\tilde{t}k\sqrt{|S_0|})\right|}{\left|C'_{(p,\beta_{-1},\beta_1)}(\tilde{t}k\sqrt{|S_0|})\right|^2} =$$
$$= 4\pi \frac{\left|S'_{(p,\beta_{-1},\beta_1)}(\tilde{t}\sqrt{|S_0'|})\right|}{\left|C'_{(p,\beta_{-1},\beta_1)}(\tilde{t}\sqrt{|S_0'|})\right|^2} = I^{S_0}_{(p,\beta_{-1},\beta_1)}(\tilde{t})$$

which concludes the proof.

Remark: We notice that in the case of the mean curvature evolution ($(p,\beta_{-1},\beta_1) = (1,-1,1)$), if $C(t)$ is a family of single Jordan curves, then, following the results of the previous section we have that

$$\left|S_{(1,-1,1)}(\tilde{t}\sqrt{|S_0|})\right| = |S_0|\left(1-\pi\tilde{t}^2\right)_+$$

so we have a close form expression for the evolution of the surface. In particular we have that since $S_{(1,-1,1)}(t)$ converges towards a circle before vanishing then $I^{S_0}_{(1,-1,1)}(\tilde{t})$ satisfies:

$$\underset{\tilde{t}\to\left(\sqrt{\frac{1}{\pi}}\right)^-}{Lim} I^{S_0}_{(1,-1,1)}(\tilde{t}) = 1.$$

On the other hand, in the case $p = 0$ we have that

$$\left|C_{(p,\beta_{-1},\beta_1)}(\tilde{t}\sqrt{|S_0|})\right| = \left(|C_0| - 2\pi\beta_1\tilde{t}\sqrt{|S_0|}\right)_+$$

so we have a close form expression for the evolution of the perimeter.

4 Morphological Affine Invariant Representation of a Shape.

We consider a general affine transformation given by

$$H(x,y) = A\begin{pmatrix} x \\ y \end{pmatrix} + \begin{pmatrix} a \\ b \end{pmatrix}$$

where A is a $2x2$ matrix with $|A| \neq 0$

In [2], it was showed that the only affine invariant morphological multiscale analysis is given by

$$\beta(s) = \begin{cases} \beta_1 s^{\frac{1}{3}} & if \quad s \geq 0 \\ \beta_{-1}(-s)^{\frac{1}{3}} & if \quad s < 0 \end{cases}$$

where $\beta_1 \geq 0$ and $\beta_{-1} \leq 0$. In this case we have that

$$H\left(T_{t'(H,t)}(f)\right) = T_t(H(f))$$

where

$$t'(H,t) = |A|^{\frac{4}{3}}\, t$$

On the other hand, given 2 bounded shapes S_0, S_0', such that there exists an affine transformation H with $H(S_0') = S_0$, we have that:

$$\left|S_{(p,\beta_{-1},\beta_1)}(\tilde{t})\right| = \frac{\left|S'_{(p,\beta_{-1},\beta_1)}(\sqrt{|A|}\tilde{t})\right|}{|A|} \quad for\ any\ t \geq 0 \tag{12}$$

In the case of the affine invariant representation, we can not use the scale-normalized isoperimetric ratio because the perimeter is not invariant under affine transformations. So we will propose a geometric invariant based just on the surface evolution. We will introduce the scale-normalized surface ratio.

Definition 6 *Let be S_0 a bounded shape, we define the scale-normalized surface ratio evolution $SR^{S_0}_{(p,\beta_{-1},\beta_1)}(\tilde{t})$ as the function*

$$SR^{S_0}_{(p,\beta_{-1},\beta_1)}(\tilde{t}) = \frac{\left|S_{(p,\beta_{-1},\beta_1)}(\tilde{t}\sqrt{|S_0|})\right|}{|S_0|}$$

Next, we will show that $SR^{S_0}_{(p,\beta_{-1},\beta_1)}(\tilde{t})$ is an affine invariant of the shape S_0.

Theorem 7 *Let $T_t^{(1,\beta_{-1},\beta_1)}(f)$ be a morphological multiscale analysis invariant under affine transformations ($p = \frac{1}{3}$), 2 bounded shapes S_0, S_0', such that there exists an affine transformation H with $H(S_0') = S_0$, Then:*

$$SR^{S_0}_{(\frac{1}{3},\beta_{-1},\beta_1)}(\tilde{t}) = SR^{S_0'}_{(\frac{1}{3},\beta_{-1},\beta_1)}(\tilde{t}) \quad for\ \tilde{t} \geq 0$$

Proof: Using (12) we obtain:

$$SR^{S_0}_{(\frac{1}{3},\beta_{-1},\beta_1)}(\tilde{t}) = \frac{\left|S_{(\frac{1}{3},\beta_{-1},\beta_1)}(\tilde{t}\sqrt{|S_0|})\right|}{|S_0|} = \frac{\left|S'_{(\frac{1}{3},\beta_{-1},\beta_1)}(\tilde{t}\sqrt{|S_0|\,|A|})\right|}{|S_0|\,|A|} =$$
$$= \frac{\left|S'_{(\frac{1}{3},\beta_{-1},\beta_1)}(\tilde{t}\sqrt{|S_0'|})\right|}{|S_0'|} = SR^{S_0'}_{(\frac{1}{3},\beta_{-1},\beta_1)}(\tilde{t})$$

which concludes the proof.

The vanishing scale.

Definition 8 *Given a morphological multiscale analysis $T_t^{(p,\beta_{-1},\beta_1)}(f)$ with $p \geq 0$ and a shape S_0, we define the vanishing scale $t_\infty^{(p,\beta_{-1},\beta_1)}(S_0)$ as the number:*

$$t_\infty^{(p,\beta_{-1},\beta_1)}(S_0) = \sup_{t>0}\{|S(t)| > 0\}$$

Remark: We notice that if $\beta_1 > 0$ and S_0 is a bounded shape, then by the inclusion principle we have that

$$S(t) \subset B_{\left(R_0^{p+1} - \beta_1 t(p+1)\right)^{\frac{1}{p+1}}}(x_0, y_0)$$

and therefore $t_\infty^{(p,\beta_{-1},\beta_1)}(S_0) < R_0^{p+1}/(\beta_1(p+1)) < \infty$.

Remark: We notice that if we use the scale $\tilde{t}$, given in (6), instead of t, then the vanishing scale for a circle of radius R_0 is given by:

$$\tilde{t}_\infty^{(p,\beta_{-1},\beta_1)}(B_{R_0}(x_0, y_0)) = \beta_1^{\frac{1}{p+1}} R_0$$

On the other hand, under the action of a similarity or affine transformation $H()$ we have that $\tilde{t}_\infty^{(p,\beta_{-1},\beta_1)} \to k\tilde{t}_\infty^{(p,\beta_{-1},\beta_1)}$,where k is the scaling factor of the similarity or $\tilde{t}_\infty^{(p,\beta_{-1},\beta_1)} \to \sqrt{|A|}\tilde{t}_\infty^{(p,\beta_{-1},\beta_1)}$ in the case of an affine transformation. This relations provides to us another way to normalize the scale in the scale-normalized isoperimetric ratio and the scale-normalized surface ratio, in other words the following functions are similarity (respect. affine) invariant of a shape

$$I^{S_0}_{(p,\beta_{-1},\beta_1)}(\tilde{t}) = \frac{\left|S_{(p,\beta_{-1},\beta_1)}(\tilde{t}(\tilde{t}_\infty^{(p,\beta^*_{-1},\beta^*_1)}))\right|}{\left|C_{(p,\beta_{-1},\beta_1)}(\tilde{t}(\tilde{t}_\infty^{(p,\beta^*_{-1},\beta^*_1)}))\right|^2}$$

$$SR^{S_0}_{(\frac{1}{3},\beta_{-1},\beta_1)}(\tilde{t}) = \frac{\left|S_{(\frac{1}{3},\beta_{-1},\beta_1)}(\tilde{t}(\tilde{t}_\infty^{(\frac{1}{3},\beta^*_{-1},\beta^*_1)}))\right|}{\left(\tilde{t}_\infty^{(\frac{1}{3},\beta^*_{-1},\beta^*_1)}\right)^2}$$

so we can compute $\tilde{t}_\infty^{(p,\beta^*_{-1},\beta^*_1)}$ for a particular choice of (β^*_1,β^*_{-1}) and then we can normalize the scale with $\tilde{t}_\infty^{(p,\beta^*_{-1},\beta^*_1)}$ for any other multiscale analysis (β_1,β_{-1})

5 Numerical Experiences

The numerical algorithms that we use to approach numerically the morphological multiscale analysis that we use, are based in the techniques studied in [3]. First, we will present some experiences using the scale normalized isoperimetric ratio evolution $I^{S_0}_{(1,\beta_{-1},\beta_1)}(\tilde{t})$. We will use some synthetic shapes given in figure 1. All the shapes (except the circle) have similar initial isoperimetric ratio (in fact theoretically the isoperimetric ratio is exactly the same for all shapes, however, in practice, because of pixel noise and numerical errors, the computed isoperimetric ratio is not the same). The shapes are organized as follow: For each shape we have evaluated a similarity transformation where we have rotated and changed the size of the original shape. So shapes $1-2$, $3-4$, $4-5$, $5-6$ and $7-8$ are equivalent modulus a similarity transformation. Shape 9 is similar to shape 7 but in shape 9, we have changed the location of the inside square. We will compare $I^{S_0}_{(1,\beta_{-1},\beta_1)}(\tilde{t})$ for the different shapes for $\tilde{t} \in [0, 0.3]$. We remember that

$$\lim_{\tilde{t}\to\left(\sqrt{\frac{1}{\pi}}\right)^-} I^{S_0}_{(1,-1,1)}(\tilde{t}) = 1.$$

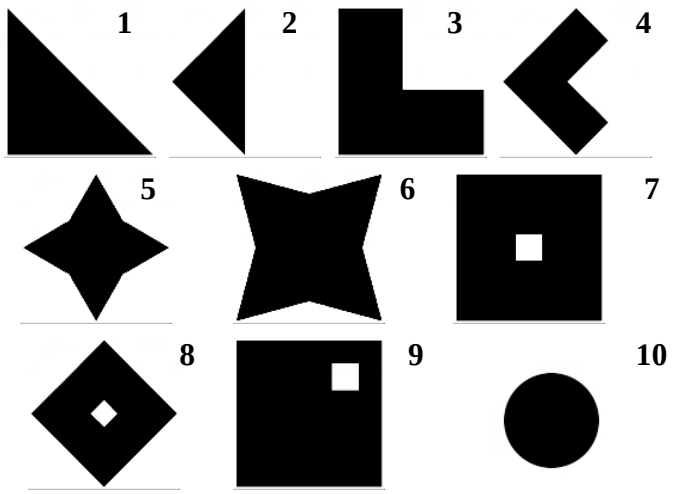

Figure 1: Test shapes used to evaluate the scale-normalized isoperimetric ratio.

Therefore $\tilde{t} = \sqrt{\frac{1}{\pi}} \simeq 0.56$ is the upper bound for the scale comparison.

In figure 2, we present the evolution of $I^{S_0}_{(1,-1,1)}(\tilde{t})$ for the shapes of figure 1. Each shape has associated several graphs which correspond to the evolution of $I^{S_0}_{(1,-1,1)}(\tilde{t})$ for the different transformations of the shapes. So we can realize that following the evolution of $I^{S_0}_{(1,-1,1)}(\tilde{t})$ we can discriminate very well between the different shapes. We notice that shapes $7-8-9$ have similar evolutions because the evolution of $I^{S_0}_{(1,-1,1)}(\tilde{t})$ is not altered by the location of the inside square.

In figure 3, we present the evolution of $I^{S_0}_{(1,0,1)}(\tilde{t})$ for the shapes of figure 1. We notice that in this case, shapes 7 and 9 have different evolution following the location of the inside square. This behavior is illustrated in figure 4 where we show some steps of the evolution of $S_{(1,0,1)}(t)$ across the scales for shape 9.

In figure 5, we present the evolution of $I^{S_0}_{(1,0,1)}(\tilde{t})$ for the shapes of figure 1.

Next, we will present some experiences using the scale normalized surface ratio evolution $SR^{S_0}_{(\frac{1}{3},\beta_{-1},\beta_1)}(\tilde{t})$. We will use some synthetic shapes given in figure 6. For each shape we have evaluated an affine transformation where we have changed the horizontal and vertical sizes in a different way. So shapes $1-2$, $3-4$, $4-5$, $5-6$, $7-8$ and $9-10$ are equivalent modulus an affine transformation. We will compare $SR^{S_0}_{(\frac{1}{3},\beta_{-1},\beta_1)}(\tilde{t})$ for the different shape for $\tilde{t} \in [0, 0.3]$.

In figure 7, we present the evolution of $SR^{S_0}_{(\frac{1}{3},-1,1)}(\tilde{t})$ for the shapes of figure 6.

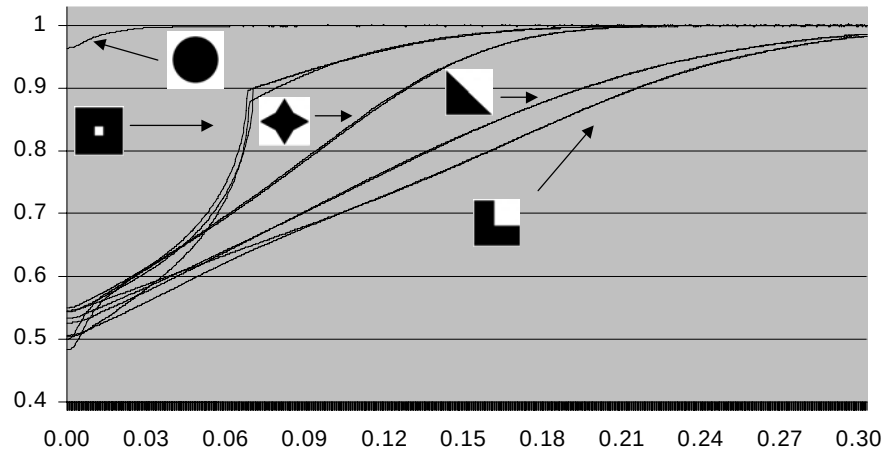

Figure 2: Evolution of $I^{S_0}_{(1,-1,1)}(\tilde{t})$ for the shapes of figure 1.

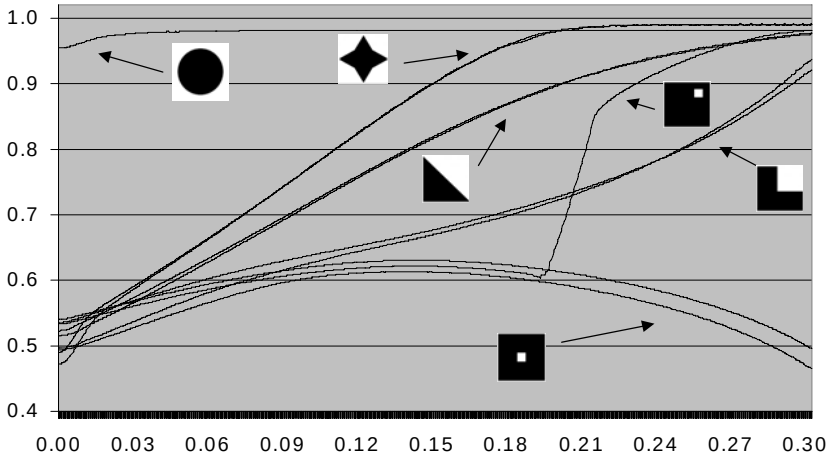

Figure 3: Evolution of $I^{S_0}_{(1,0,1)}(\tilde{t})$ for the shapes of figure 1.

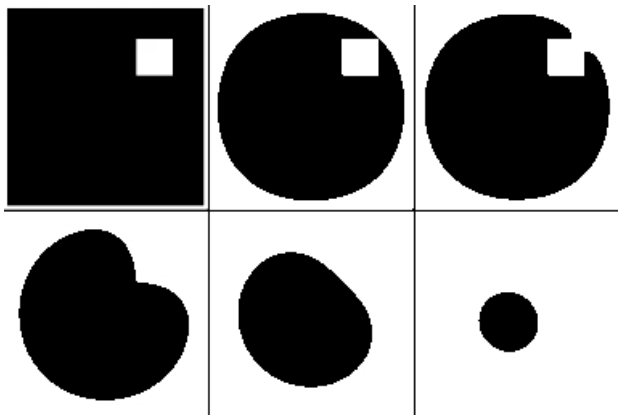

Figure 4: From left to right and from top to down: Evolution of $S_{(1,0,1)}(\tilde{t})$ for shape 9 of figure 1.

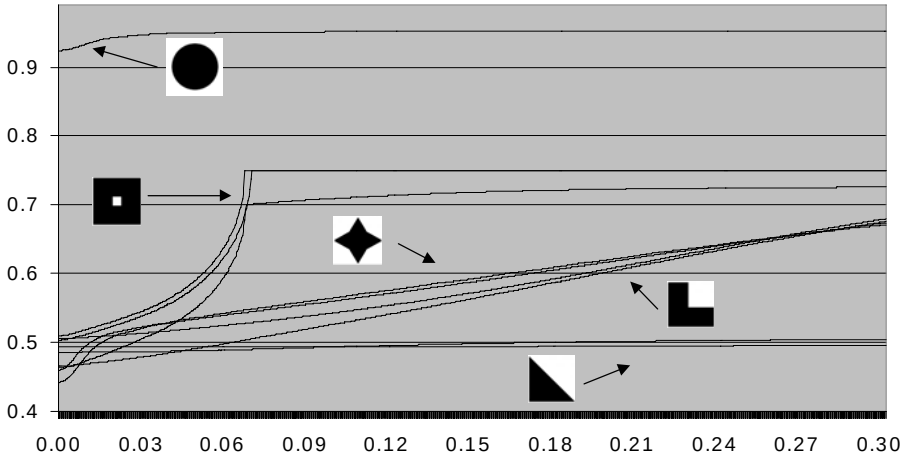

Figure 5: Evolution of $I^{S_0}_{(1,-1,0)}(\tilde{t})$ for the shapes of figure 1.

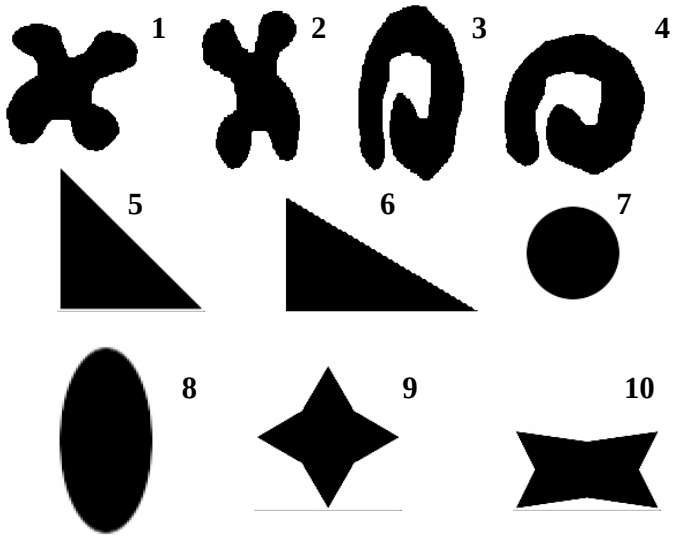

Figure 6: Test shapes used to evaluate the affine invariant scale-normalized surface ratio evolution

Each shape has associated 2 graphs which correspond to the evolution of $SR^{S_0}_{(\frac{1}{3},-1,1)}(\tilde{t})$ for the different transformations of the shapes.

In figure 8, we present the evolution of $SR^{S_0}_{(\frac{1}{3},0,1)}(\tilde{t})$ for the shapes of figure 6. We notice that in this case, only the convex region of the shape evolves, so this behavior produces a strong discrimination between the evolution of shapes following the geometry of their convex and concave regions. This effect can be observed if we compare the evolution of shapes 3 and 7. The evolution of $SR^{S_0}_{(\frac{1}{3},0,1)}(\tilde{t})$ for these 2 shapes is very different, but the evolution of $SR^{S_0}_{(\frac{1}{3},-1,1)}(\tilde{t})$ for the same shapes are much more similar. So in practice, it means that using the information of the surface evolution with different values of β_{-1} and β_1 we obtain a better discrimination power between different shapes.

In figure 8, we present the evolution of $SR^{S_0}_{(\frac{1}{3},-1,0)}(\tilde{t})$ for the shapes of figure 6. The evolution with the multiscale analysis $T_t^{(\frac{1}{3},-1,\mathbf{0})}$ is more sensitive to pixel noise than the ones corresponding to $\beta_1 > 0$. The reason is that in this case we have not a regularization effect on the boundary. This behavior can be observed in this numerical experience: For instance the evolution of the triangles given by shapes 5 and 6 are

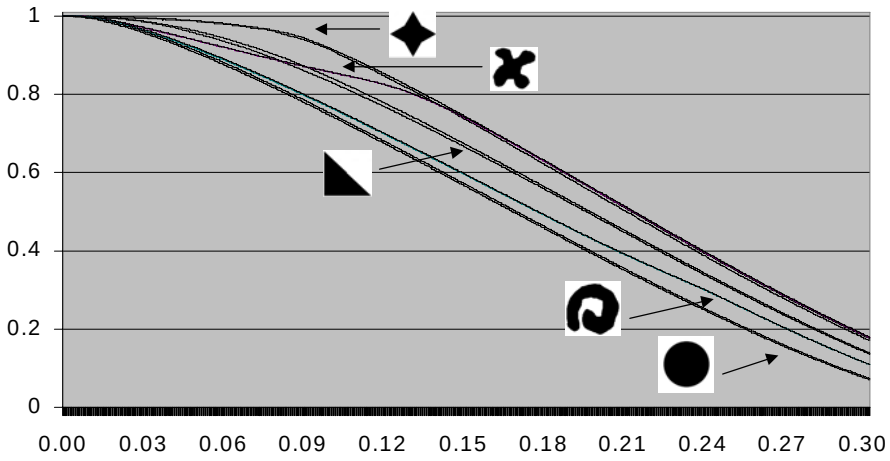

Figure 7: Evolution of $SR^{S_0}_{(\frac{1}{3},-1,1)}(\tilde{t})$ for the shapes of figure 6.

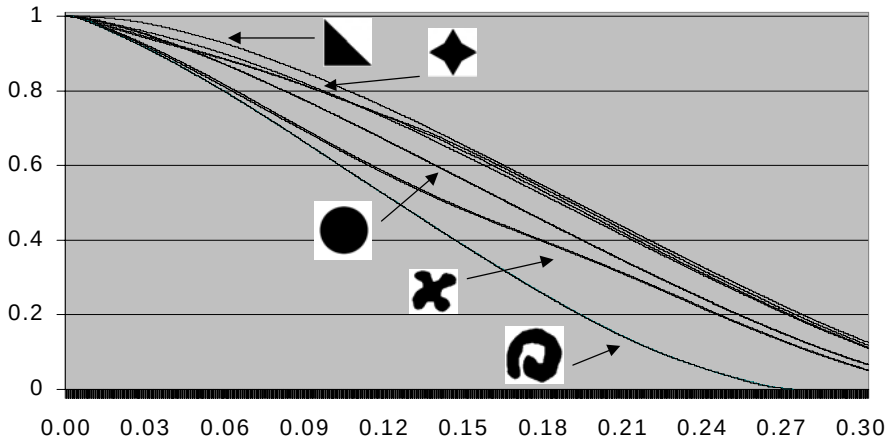

Figure 8: Evolution of $SR^{S_0}_{(\frac{1}{3},0,1)}(\tilde{t})$ for the shapes of figure 6.

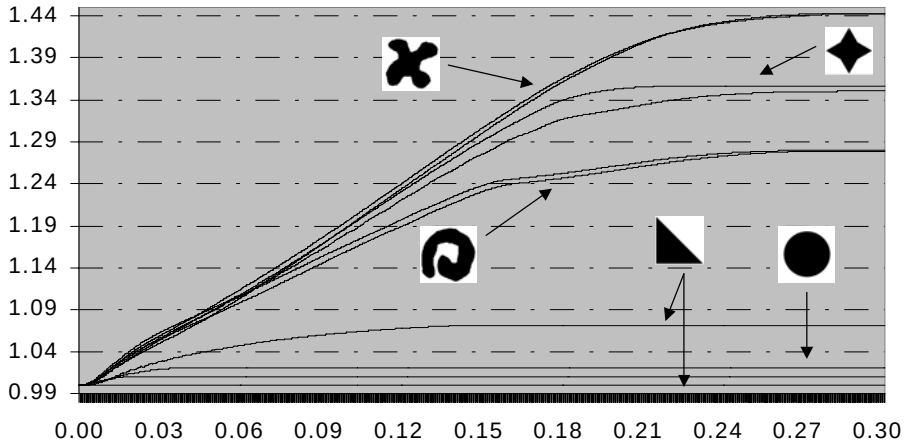

Figure 9: Evolution of $SR^{S_0}_{(\frac{1}{3},-1,0)}(\tilde{t})$ for the shapes of figure 6.

quite different because of some pixel errors introduced by the application of the affine transformation to shape 5.

6 Conclusions

In this paper, we have presented a new geometric invariant shape representation using morphological multiscale analysis. The geometric invariant is based on the surface and perimeter evolution of the shape under the action of a morphological multiscale analysis.

We have introduced a similarity invariant shape representation based on a scale-normalized isoperimetric ratio evolution. In this case we have focused our attention in the morphological multiscale analysis generated by the mean curvature motion evolution. In order to increase the discrimination power of the shape representation, we propose to combine the information of the evolution of shapes using different values of β_{-1} and β_1. In this way we can discriminate between the convex and concave regions of the shapes. We have presented some numerical experiences and the results are very promising.

In the case of general affine geometric transformations the proposed geometric invariant is based on a scale-normalized evolution of the surface using the affine invari-

ant morphological multiscale analysis $T_t^{(\frac{1}{3},\beta_{-1},\beta_1)}$. We have presented some numerical experiences and the results are also very promising.

Acknowledgments. This work has been supported by the European TMR network *Viscosity Solutions and their Applications.*

References

[1] L. Alvarez, A.P. Blanc, L. Mazorra and F. Santana, *Geometric flows and global invariant signatures*, Cuadernos del Instituto Universitario de Ciencias y Tecnologías Cibernéticas Vol. 15, 1–23, 2001

[2] L. Alvarez, F. Guichard, P.-L. Lions and J.-M. Morel, *Axioms and fundamental equations in image processing*, Arch. Rational Mech. Anal., Vol. 123, 199–257, 1993.

[3] L. Alvarez and J.M. Morel, *Formalization and Computational Aspects of Image Analysis,* Acta Numerica pp. 7-59, 1994.

[4] H. Asada and M. Brady. The curvature primal sketch, IEEE Transactions on PAMI, Vol. 8, 2-14, 1986

[5] T. Cohignac and C. Lopez and J. M. Morel, *Integral and local affine invariant parameter and application to shape recognition*, Proceedings of ICPR conference, A:164–168, 1994.

[6] T. Cohignac and J. M. Morel, *Scale space and affine invariant recognition of occluded shapes*, Proceedings of Spie conference, investigate and trial image processing, Vol. 2567, 214–222, 1995.

[7] J.L. Lisani, L. Moisan, P. Monasse, and J.M. Morel. *Affine invariant mathematical morphology applied to a generic shape recognition algorithm.* In Mathematical Morphology & its Applications to Image & Signal Process. Vol. 18. Kluwer Academic Publishers.

[8] S. Loncaric. *A Survey of Shape Analysis Techniques.* Pattern Recognition, Vol. 31, No. 8, pp. 983-1001, 1998

[9] P. Maragos. *Pattern spectrum and multiscale shape representation.* IEEE Transactions on Pattern Analysis and Machine intelligence, 11(7):701-716, July 1989.

[10] Mokhtarian, F. and A. K. Mackworth, *A Theory of Multi-Scale, Curvature-Based Shape Representation for Planar Curves*, IEEE Trans. Pattern Analysis and Machine Intelligence, vol. 14, no. 8, pp. 789-805, 1992.

[11] T. Pavlidis, *A review of algorithms for shape analysis*, Computer Graphics Image Processing, vol. 7, pp. 242–258, 1978.

[12] G.Sapiro and A.Tannenbaum, *Affine invariant scale space*, International Journal of Computer Vision, Vol 11, 25–44, 1993.

[13] A. Witkin. *Scale space filtering:A new approach to multi-scale description.* In S. Ullman and W. Richards, editors, Image Understanding 1984, Ablex, New Jersey, 1984.